

Hydrogen adsorption on Al(100)

J. Paul

Corporate Research Science Laboratories, Exxon Research and Engineering Company, Route 22 East, Annandale, New Jersey 08801

(Received 11 June 1987; revised manuscript received 5 November 1987)

Adsorption studies of hydrogen and deuterium on the clean (100) surface of aluminum are reported. The probability for H_2 (D_2) dissociation and subsequent metal-hydrogen bond formation is less than $1:10^4$. This prompted the use of a beam of atomic hydrogen (deuterium). We have adsorbed between 0.01 and 1.0 monolayer and studied annealing sequences between 80 and 750 K with electron-energy-loss spectroscopy (EELS) and thermal-desorption spectroscopy (TDS). At <90 K we observe surface hydrogen coordinated in bridge positions, characterized by an Al-H (-D) vibrational band at 1125 (800) cm^{-1} . Annealing to 150 K causes dominant features to appear at 1750 (1250) and 750 (550) cm^{-1} . These losses are interpreted as the stretching and bending and/or scissoring modes of a terminally coordinated species. Further annealing to 280 K sees the growth of an intense band at 1825 (1325) cm^{-1} , with no correlated low-frequency band. This last annealing signals the formation of another terminally coordinated species, tentatively assigned as " $p(1 \times 1)$ islands." Hydrogen recombination and molecular desorption is observed between 340 and 360 K. We have no indication of any scattering resonance in the elastic energy range 1–9 eV, nor do the angular profiles of the above losses deviate from the profile of the elastic peak. All vibrational modes are thus concluded to be dominated by dipole excitations.

I. INTRODUCTION

Hydrogen adsorbed on aluminum and the formation and decomposition of Al—H bonds is interesting from both theoretical and technological aspects. The interaction visualizes a puritanical chemisorption system at the same time, as the hydride was considered a potential rocket propellant, and hydrogen-filled cavities cause mechanical weakness and virtual leaks in aluminum vessels.¹ In the electronics manufacturing industry both hydrogen and aluminum are used routinely.² Despite these diverse and strong incentives, surface-science studies are not abundant.³⁷ The probability for hydrogen-bond breaking on the flat surface is infinitely small and hydrogen must therefore either be implanted at high velocities or be supplied as a beam of atoms. The latter can be accomplished with a hot tungsten filament, a method which can become acceptable if the stirring of molecules in the experimental chamber is kept at a minimum.

In contrast to the inertness of the flat surface, aluminum atoms¹⁸ and clusters⁹ react with hydrogen gas. With this experimental evidence at hand, care should be exercised when applying results of even elaborate cluster models to hydrogen chemisorption on bulk aluminum.^{10,11} Application of quantum-chemical cluster models to surface events is probably better justified for the dissociative adsorption in the presence of $d\pi$ orbitals.¹² Aluminum is a realization of a free-electron metal and, consequently, is not armed with a partly filled d band, but is well suited for the smooth background or jellium substrate model.^{13–15} Such calculations have concluded that atomic hydrogen readily penetrates a low-electron-density material (Na), but bounces off a high-density material (Al), except for a shallow bound state at the vacuum tail of diminishing electron density.¹⁶ Electron-

density minima provide stabilized binding sites for hydrogen atoms forced into bulk aluminum. Such minima can be found at point defects (vacancies, contaminants, etc.) or can be created by a lattice expansion.^{17–23} The surfaces of internal cavities or "bubbles" also provide preferred binding sites. The effective-medium theory provides a cost-effective way of seeking the most suitable electron density for hydrogen chemisorption.²⁴

Aluminum and hydrogen can form a microcrystalline bulk hydride, AlH_3 .²⁵ The geometry of the Al atoms in the densest layer is the same as that in the metal, except that the Al-Al distance in AlH_3 is 4.45 \AA and in Al metal it is 2.86 \AA .²⁶ This very unstable hydride²⁷ may be seen as the extreme consequence of hydrogen absorbed at sites of preferred electron density.

Being the interface between molecular and solid-state physics, surface science grasps at the best of each world. Above we learned about hydrogen sites in solid aluminum and crystalline aluminum hydride, AlH_3 . Below we will discuss gas-phase studies of the metal evaporated into hydrogen gas. Aluminum vapor condensation in a hydrogen atmosphere is an established procedure to prepare a film of aluminum hydride.²⁸ Obviously, either vaporized aluminum or defect sites with low coordination numbers activate H—H bonds. Cox *et al.* narrowed the discussion by producing a beam of aluminum clusters with a well characterized size distribution.⁹ They found a peak in hydrogen dissociation activity for Al_6 . Upton explained this result as the interaction between unique cluster d orbitals and hydrogen.¹⁰ Substrate orbitals of d symmetry are apparently essential for dihydrogen activation.

The present work is an effort to characterize hydrogen adsorption on aluminum. In the Sec. III we discuss the following: (A) thermal-desorption data for Al(100), (B)

the identities of vibrational losses, (C) influence of surface modifications, (D) excitation profiles, (E) coverage dependence, (F) temperature dependence, and (G) the nature of a puzzling species with vibrations around 1750 and 750 cm^{-1} . The discussion will benefit from our previous adsorption studies on aluminum.²⁹⁻³³ A forthcoming paper will discuss the attractive interaction between co-adsorbed hydrogen and alkali atoms and the formation of alkali hydrides.³⁴

II. EXPERIMENT

Experiments were carried out in a stainless-steel ultrahigh-vacuum (UHV) chamber equipped for a variety of surface spectroscopies and operated at 1×10^{-10} Torr. The crystal mount and a 3-h cleaning procedure were described in an earlier communication.²⁹ Crystal cleanliness was followed with Auger-electron spectroscopy (AES) and verified with electron-energy-loss spectroscopy (EELS).²⁹

EEL spectra were measured at 5 eV primary beam energy and 60 cm^{-1} resolution (Leybold double-pass electrostatic analyzer). Work-function changes ($|\Delta\Phi| > 40$ mV) and diffraction patterns were followed with a Varian Associates low-energy electron-diffraction (LEED) unit. Thermal-desorption (TDS) spectra were recorded at 1.3 K sec^{-1} . Desorbing species were sampled with a straight, 1-in. drift tube "connecting" the sample with the mass spectrometer (UTI model 100C). Traces of the total pressure were obtained by switching off the rf field in the electron-multiplier mode. This, for instance, enabled us to confirm the absence of any desorbing species of an unknown mass with a sensitivity comparable to that of single-mass spectra. Finally, Auger spectra (Φ -Electronics single-pass cylindrical-mirror analyzer, $E_p = 3$ keV, $V_{p.p.} = 2$ V) were recorded before and after each set of spectra, i.e., not in the presence of surface hydrogen.

Initially, we tried to adsorb hydrogen from the gas phase via beam dosers directed at the crystal. This procedure had previously been used for CO with a sticking coefficient of $< 10^{-3}$.³⁰ In the case of hydrogen, however, no adsorption could be detected. The beam-doser efficiency compared with "backfilling" was calibrated to 50:1 for water,²⁹ but we only use a conservative estimate of 5:1 for hydrogen. These tests still set $1:10^4$ as an upper limit for the probability of hydrogen dissociation and adsorption on Al(100) in the temperature range 80–280 K. Consequently, hydrogen had to be supplied as a beam of atoms.

Hydrogen atoms were produced at a hot (1800-K) 5-mm-wide tungsten filament, flushed with dihydrogen from a beam doser adjacent to and directed at the filament. The crystal was positioned 100 mm from the filament and the front side exposed only after steady-state conditions were obtained—this in order to avoid any initial burst of contaminants as the filament current was increased and the beam doser opened. A "rest" current was passed through the filament at all times. The sample-to-filament distance was a compromise between radiative heating, critical because of the high mobility of hydrogen on aluminum, and a diminishing solid angle,

again critical to avoid overly high background pressures and thus sample contamination. Each "overlayer" was prepared by adsorption below 90 K, followed by flashing to a desired temperature, and recoiling to < 90 K. All dosing and annealing sequences were repeated with both H_2 and D_2 . Doses are reported in X langmuirs ($1 \text{ L} \equiv 1 \times 10^{-6}$ Torr sec), as read on the ion gauge. Calibration of hydrogen uptake versus dose and thermal-desorption traces is discussed below.

Every experiment was rounded off by a dihydrogen desorption spectrum, which provided an excellent measurement of the actual relative surface coverage. The accumulated results of all such spectra are plotted in Fig. 1. Figure 1 presents data for uptake at < 90 K, but is representative also for uptake at any other temperature < 280 K. We have not observed any hydrogen-induced diffraction pattern besides the indisputable $p(1 \times 1)$ and, consequently, LEED provided no direct reference point for absolute coverages. Primary calibration of TDS peak areas was derived instead from the decomposition of a monolayer of NaH or KH.³⁴ We assumed the formation of 1:1 alkali hydrides for ordered alkali overlayers exposed to atomic hydrogen. These studies actually provided four reference points since they involved two alkali metals and both the hydride and the deuteride. We acknowledge the trivial difference between adsorbed monoatomic species and measured diatomic molecules. The calibration against alkali hydride decomposition is

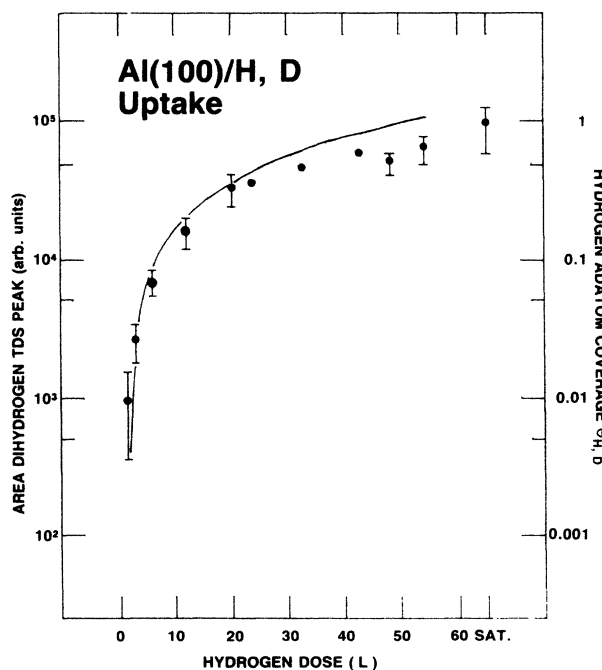


FIG. 1. Uptake of atomic hydrogen vs dose. Uptake measured as the area under the dihydrogen thermal desorption peak (m_2 or m_4). Dose given in X L, i.e., as read on the ion gauge without corrections (see Sec. II). $\Theta = 1$ denotes monolayer coverage, the derivation of which is discussed in the text. $\Theta = 1$ is used synonymously with $p(1 \times 1)$ and ML (monolayer) throughout the text. The solid line represents a least-squares linear fit in the low-dose regime (< 20 L).

utilized in Fig. 1 and throughout the text. The uptake is approximately linear with the dose for $\Theta < 0.3$, but it takes doses as high as 600 L to reach saturation. The calibration is consistent with $\Theta = 1$ as the highest coverage for hydrogen atoms with thermal velocities. The deviation from linearity may represent the physics and statistics of adsorption or coincidental saturation of the tungsten source.

Contamination levels were checked with EELS, TDS, and AES (Fig. 2). Previous titrations of oxygen and carbon coverages with reversibly adsorbed CO and alkali metals allow me to relate peak heights to actual surface coverages.^{30,31} The ratio of contamination (carbon and oxygen) to hydrogen coverage was in no case higher than 1:25, and the highest absolute contaminant coverage ever recorded was 0.04. 0.04 was observed after an accumulated hydrogen dose of > 800 L and > 6 h of experiments at LN₂ temperature. A contamination-to-hydrogen ratio of typically 1:50, which we regard as chemically insignificant, will nevertheless be visible in EELS because of the weak scattering of metal-hydrogen vibrations and the very strong scattering of aluminum-oxygen vibrations. A final contamination checkup was provided by work-function measurements. We detected no difference between the surface potential of the clean surface and the surface covered with hydrogen at < 90 K.³ No data were obtained for annealed overlayers. The resolution of these data (40 mV) does not allow any evaluation of hydrogen-induced dipole layers, but at least excludes major contamination coverages.

III. RESULTS AND DISCUSSION

A. Hydrogen adsorption and desorption

Figures 3(a) and 3(b) show recombination and desorption of hydrogen and deuterium on Al(100) between 340 and 360 K. The temperature range is about the same as for Cu(111) (Ref. 35) and Zn(0001) (Ref. 36), but lower than on most transition metals (Refs. 37 and 38). The presence of *d* states at the Fermi level and thus the ability to promote H—H bond breaking appears to go hand in hand with relatively high desorption temperatures. This is further illustrated in a subsequent article where we discuss the stability of adsorbed hydrogen in the presence of co-adsorbed alkali atoms.³⁴

It appears as if the desorption temperature shifts to higher values at coverages above $\Theta = 0.5$, but hardly at all below this density. The slightly higher temperature observed at $\Theta < 0.02$ probably has little significance for hydrogen adsorbed on the flat surface, but instead indicates adsorption at unspecified defect sites. The increased stability at the highest coverages comes when the average hydrogen atom is experiencing an almost complete coordination shell of neighboring hydrogen atoms. The higher temperature may then indicate either a deepened chemisorption potential induced by adjacent atoms or simply the blocking of rendezvous. The effect of a full coordination shell will be illuminated when we discuss the vibrational spectra of annealed hydrogen "*p*(1×1) islands." We do not consider the difference between the lower limits for hydrogen (345 K) and deuteri-

um (340 K) desorption as significant and conclude, consequently, that no isotopic shift has been detected. This is consistent with the idea that we are probing a minor isotopic shift caused by diffusion rather than by bond dissociation.³⁹

The present results will also illuminate previous data on water decomposition and hydrogen evolution on

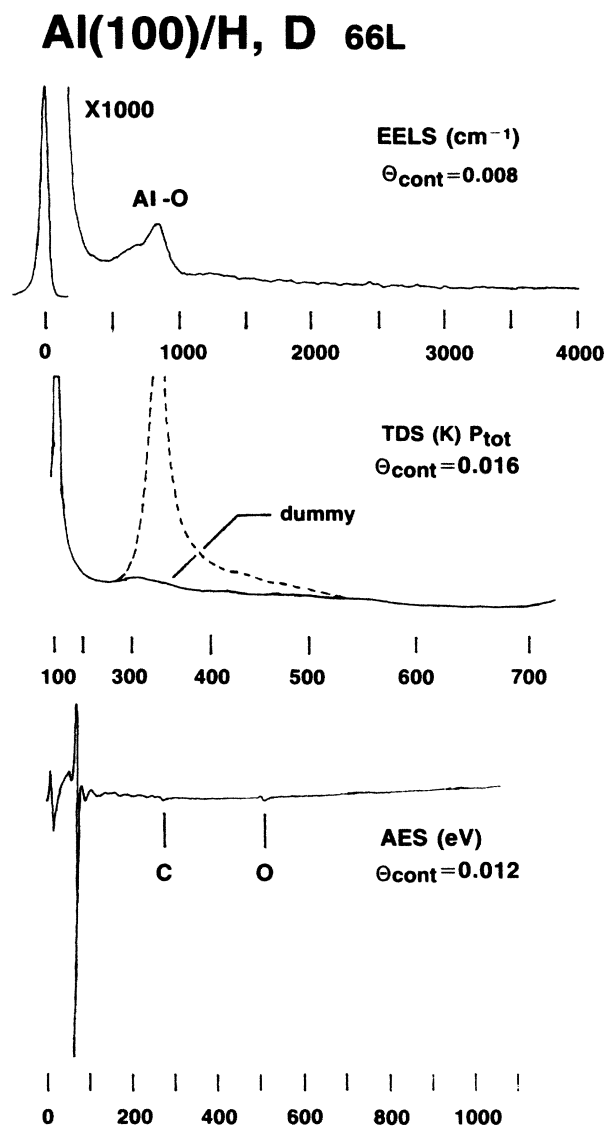


FIG. 2. Surface contamination as measured with EELS, TDS, and AES. Each surface was exposed to 66 L at < 90 K (see Sec. II). The EEL spectrum was obtained after flashing to > 700 K. The contamination peak corresponds to around 0.008 of a monolayer of aluminum oxide (Ref. 30). The TDS spectrum was obtained with (dashed line) or without (solid line, "dummy") the crystal facing the hot W filament. Both curves represent the total pressure (see Sec. II). $\Theta = 0.016$ represents the area under all small bumps in the solid line. The AES spectrum represents an analysis after flashing to 700 K (cf. EELS). The relative magnitude of the carbon and the oxygen peaks correspond to a contamination coverage of around 0.012 (Refs. 30 and 31).

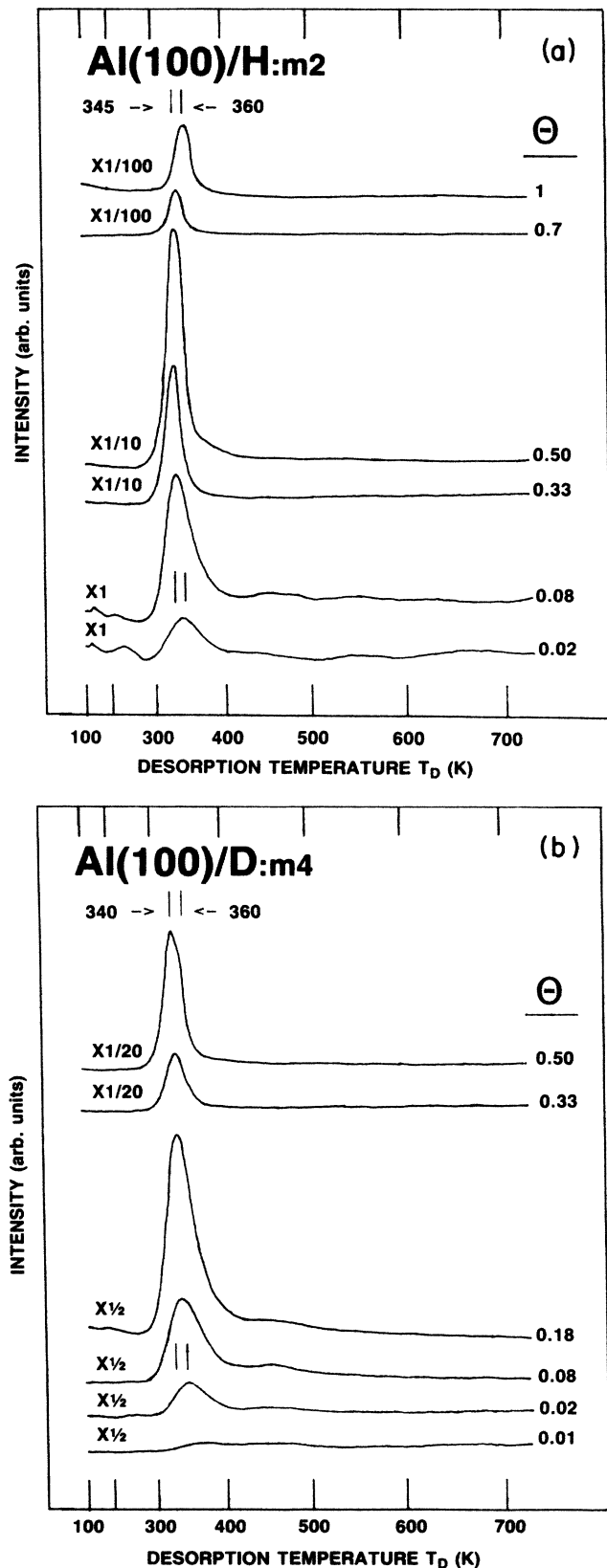


FIG. 3. Thermal-desorption spectra of dihydrogen [(a) m_2 or (b) m_4 when recombined] as a function of exposure. The coverage refers to atomic hydrogen (deuterium). The difference between 340 K (D) and 345 K (H) as the lower limit is hardly significant, and we do not conclude any observed isotope effect.

aluminum. Following water decomposition, Paul and Hoffmann observed H_2 (D_2) desorption at around 140 (180) K.²⁹ The 40-K isotopic shift reveals a process limited by O—H bond breaking. Moreover, the overall much lower desorption temperature compared with hydrogen recombination on the clean surface (this work) rules out the possibility that hydrogen atoms from water dissociation occupy unmodified adsorption sites on the metal. An ongoing study will investigate whether it is sufficient to consider metal-hydrogen-bond weakening caused by co-adsorbed oxygen atoms or hydroxyl groups to explain the low desorption temperature.⁴⁰ An alternative proposal is that intermolecular hydrogen bonding must be included in any relevant model of water decomposition⁴¹ and that no intermediate state with adsorbed hydrogen atoms will ever exist.

Several studies deal with the diffusion of hydrogen in bulk aluminum and hydrogen evolution after ion implantation.^{42–46} Care has to be exercised when absorbing these data, since surface cleanliness will affect hydrogen recombination.^{29,34} Myers *et al.* observed hydrogen evolution at 340 K from a freshly sputtered aluminum sample implanted with deuterium.⁴⁵ The release of hydrogen was believed to be linked to the annealing of “traps” close to the surface. Observing Figs. 3(a) and 3(b), one is inclined to believe that surface recombination is the limiting factor in hydrogen evolution from bulk aluminum. The omission of sputtering shifted the desorption of implanted hydrogen to approximately 150 K higher temperature.⁴⁵ The difference was attributed to the presence of an oxide barrier at the surface. We have previously observed a stable metal/oxide “interfacial hydride” after flashing to 650 K, which nicely translates into a surface barrier for recombination.²⁹

B. Identification of vibrational losses

Figure 4 displays our procedure to ensure the relevance of observed vibrational losses. The dominant band at <90 K comes at 1125 cm^{-1} for hydrogen and 800 cm^{-1} for deuterium. At this temperature we also observe a band at around 600 cm^{-1} for both deuterium and hydrogen. This band is marked C for contamination. A third minor band at the high-frequency shoulder of the dominant $1125\text{--}(800\text{--})\text{ cm}^{-1}$ peak shifts with isotopic substitution, as does a fourth band at $1750\text{ (1250)}\text{ cm}^{-1}$. The band at $1750\text{ (1250)}\text{ cm}^{-1}$ multiplies in intensity following annealing to 150 K. This annealing also causes a band to appear at $750\text{--}(550\text{--})\text{ cm}^{-1}$ wave numbers. The band for hydrogen at 750 cm^{-1} is considerably stronger than the corresponding band for deuterium at 550 cm^{-1} . Again we are forced to use the abbreviation C for contamination contribution. Finally, as we anneal to 280 K the dominant feature becomes a sharp band at $1825\text{ (1325)}\text{ cm}^{-1}$. The combination of bands at $750\text{ (550)}\text{ cm}^{-1}$ and $1750\text{ (1250)}\text{ cm}^{-1}$ still persists at this temperature, but with reduced intensity. Further annealing causes hydrogen recombination and desorption [Figs. 3(a) and 3(b)].

The ratios between hydrogen and deuterium frequencies are 1.41 ($1125/800$), 1.40 ($1750/1250$), 1.36

(750/550), and 1.38 (1825/1325). These values slightly below $\sqrt{2}$ fully justify the assignment of these vibrations to hydrogen- or deuterium-containing species. The C-marked band at 600 cm^{-1} is typical for aluminum-oxygen species at low temperature and low coverage.⁴⁷ Annealing causes this band to shift to higher frequencies and unfortunately to overlap with the Al-H band at 750 cm^{-1} . The C-marked bands correspond to less than 0.01 of a monolayer and are regarded as superimposed on the hydrogen spectra.

The band at 1750 cm^{-1} falls into the region of known Al-H stretching vibrations of terminally coordinated hydrogen atoms. Huber and Herzberg quote 1683 cm^{-1} for the ground state of the diatomic neutral molecule and 1620 cm^{-1} for the AlH^+ ion.⁴⁸ AlH_4^- shows an infrared-active band at 1740 cm^{-1} .⁴⁹ Finally, solid AlH_3 gives a broad absorption band from around 1600 to around 1900 cm^{-1} .^{50,51} No experimental data for hydrogen vibrations on the clean surface have been reported. Calculations, however, predict an isolated hydrogen atom

in a terminal position to vibrate at 1695 cm^{-1} .⁵² As a consequence of the above data, we assign the 1750 -(1250 -) cm^{-1} band to terminally coordinated "isolated" hydrogen (deuterium) atoms.

Nyberg and Tengstål, Nordlander and Holmström, and Karlsson *et al.* have reported coverage-dependent upward vibrational shifts for hydrogen adsorbed on Ni(100) and Pd(100).⁵³⁻⁵⁵ Experiments showed a 95-cm^{-1} positive shift with coverage, and theory explained this as the difference between an isolated species and the collective vibration of a saturated monolayer. The dominant cause of this shift was explained as indirect electronic effects caused by distortions of the electron density rather than a combination of "chemical effects" and dipole-dipole interactions, as is the case for CO. The sign and magnitude of the difference between the bands at 1750 and 1825 cm^{-1} (Fig. 4) correlate well with the above literature data. Hence, the band at 1825 (1325) cm^{-1} was assigned to ordered structures of terminally coordinated hydrogen atoms. These structures are tentatively described as " $p(1 \times 1)$ islands." We conclude that annealing to 280 K will promote the condensation of hydrogen clusters much in the same way as was observed for CO on metal surfaces⁵⁶ and for H on Mo(100).⁵⁷

The intensity of the band at 750 cm^{-1} parallels the intensity of the band at 1750 cm^{-1} (also see Secs. III E and III F). The value 750 cm^{-1} agrees nicely with literature data for Al-H bending or deformation modes. AlH_4^- shows, in addition to the stretching band at 1740 cm^{-1} , an ir-active bending mode at 764 cm^{-1} .⁴⁹ For bulk AlH_3 , the band at 1600 - 1900 cm^{-1} is accompanied by deformation modes around 750 cm^{-1} .^{50,51}

Finally, we have to address the band at 1125 (800) cm^{-1} . AlH_4^- has now exhausted its possibilities, but bulk AlH_3 still has some hidden aspects. The solid hydride displays an intense band at 1025 cm^{-1} , shifting to 754 cm^{-1} upon deuteration.⁵¹ Furthermore, calculations predict a frequency round 1050 cm^{-1} for hydrogen adsorbed in twofold bridge positions.⁵² We assign the 1125 -(800 -) cm^{-1} band to hydrogen bound at such sites. The vibrational bands of bridge-bonded hydrogen atoms come in pairs. The ratio between the parallel and perpendicular bands ranges from 1:1 to 1:2 and can be used to determine bond angles.⁵⁸ Any second band in the range 500 - 1125 (400 - 800) cm^{-1} is significantly less intense than the 1125 - (800 -) cm^{-1} band. This gives a hint about the excitation mechanism since only the totally symmetric perpendicular mode is excited by z-polarized light and is thus dipole active on a metal surface (cf. Sec. III D).

Tentative assignments of observed vibrational bands are as follows: 1825 cm^{-1} to ordered islands of terminally coordinated hydrogen atoms 1750 and 750 cm^{-1} to isolated terminally coordinated atoms, and 1125 cm^{-1} to bridge-bonded hydrogen. The nature of the 1750 - and 750-cm^{-1} species will be further discussed in a separate section.

C. Chemical modifications

Surface scientists do report some data for aluminum hydrogen vibrations, but only at sites modified by alumi-

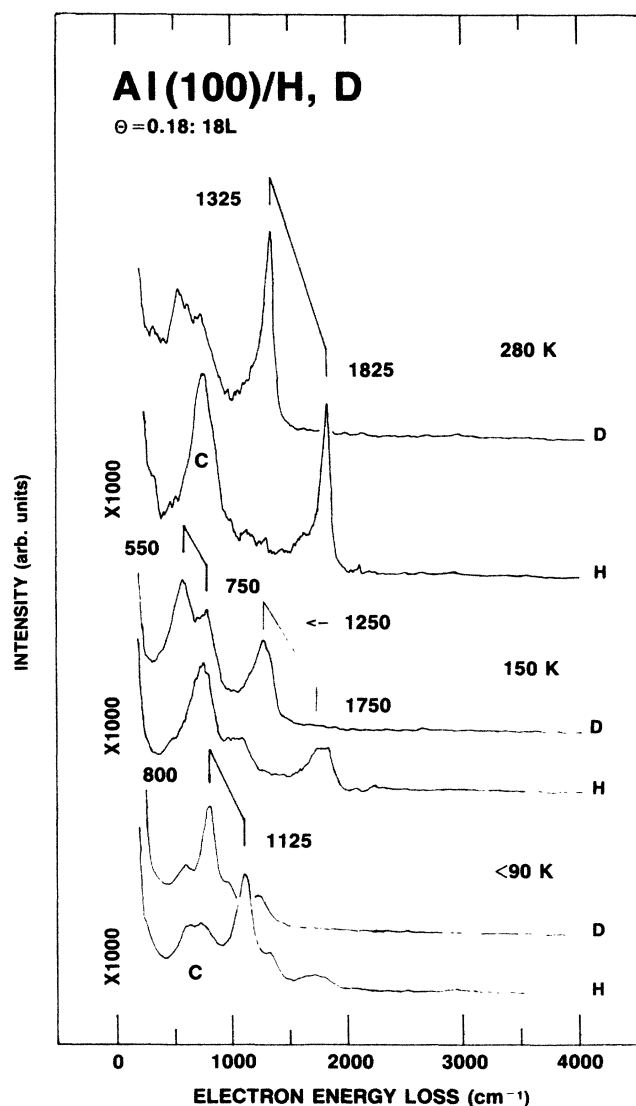


FIG. 4. Identification of hydrogen-induced vibrational bands. C denotes nonrelevant bands caused by contamination.

num oxide. Inelastic-electron-tunneling spectroscopy⁵⁹ measured Al-H vibrations at the metal-oxide interface at 1850 cm^{-1} .^{60,61} Thiry *et al.* observed an EELS band at $1895\text{--}1930\text{ cm}^{-1}$ after spraying a partly oxidized surface with hydrogen atoms.⁶² Finally, Paul and Hoffmann showed that an “interfacial hydride” band at 1910 cm^{-1} is obtained also after decomposition of surface hydroxyl groups.²⁹ Infrared matrix-isolation studies show that the addition of an hydroxyl ligand will shift the Al-H band from around 1743 cm^{-1} to around 1935 cm^{-1} .⁶³ These experimental data, plus above-quoted calculations,⁵⁴ conclusively show that the removal of electron density from the aluminum atom will raise the Al—H stretching vibration. This supports the idea of a relatively ionic aluminum-hydrogen bond. The high-temperature stability of the interfacial hydride, it persists flashes to 650 K ,²⁹ indicates a stabilized Al—H bond. Despite the above data, we advise caution for any general conclusion about the metal-hydrogen bond strength because of the complexity of the hydrogen recombination process at Al/ AlO_x sites.

Traditionally, we make surfaces “electron rich” by alkali additives. Recent data on aluminum show that the hydrogen-substrate bond is strengthened by potassium or sodium promoters.³⁴ The desorption temperature of hydrogen increases with the alkali coverage from 350 K (clean Al) to 500 K (alkali hydride decomposition). EEL spectra are dominated by intense alkali-hydrogen or alkali modified aluminum-hydrogen vibrations. Hydrogen adsorbed on Al(100) $c(2\times 2)$ Na shows a split stretching band at 1850 and 1715 cm^{-1} , a deformation mode at 800 cm^{-1} , and a metal-metal mode at 200 cm^{-1} . Exchanging sodium for potassium lowers the split high-frequency band to 1650 and 1500 cm^{-1} , and the deformation mode to 775 cm^{-1} . The metal-metal band is not observed for the potassium modified surface. From the above data it should be obvious that EELS as well as TDS can distinguish between hydrogen adsorbed on the clean aluminum surface and hydrogen adsorbed at oxygen or alkali modified sites.

D. Excitation profiles

Figure 5 displays intensity variations for the previously identified vibrations. We found that the band at 1750 (1250 cm^{-1}) becomes asymmetric at 150 K because of the growing intensity of the 1825-cm^{-1} band. We therefore introduce 130 K as the optimal annealing temperature for this band. We see that the intensities of hydrogen and deuterium bands overlap very well, except for the 750 - (550-cm^{-1}) band, where the hydrogen band appears to be more intense. This is artificial and caused by the overlapping oxygen contamination band. The left-hand panel of Fig. 5 shows that the angular profiles of all vibrations parallel the behavior of the elastic beam. The right-hand panel shows that no resonance was detected in the elastic energy range $1\text{--}9\text{ eV}$. As a consequence of the results in Fig. 5, we conclude that all vibrations are dominated by dipole scattering. Intensities of EEL spectra are not straightforward to interpret, but it appears that aluminum hydrogen vibrations are at least 1 order of magnitude more intense than typical transition-metal hydrogen

bands.^{64,65} Our limited work-function measurements did not reveal any hydrogen-induced static dipole moment that could be linked to the observed strong dynamical dipole moments. Nevertheless, we empirically note that a higher degree of ionicity in the metal-hydrogen bond, transition metals < aluminum < alkali metals, correlates well with observed loss intensities.

Somewhat puzzling is that the 750 - (550-cm^{-1}) band, assigned to Al—H bending, is apparently dipole active.⁶⁶ Assuming a correct assignment to terminally coordinated species and untampered profile measurements, we are left with only speculations for the cause of this. The 1750 - and 750-cm^{-1} states may be associated with unspecified defect sites and thus do not acknowledge surface selection rules. An alternative explanation is that we observe the A_1 symmetric stretching and scissoring modes of an H-Al-H species. Some support for this hypothesis may be gained from the literature, where the bands of AlH_4^- (764 cm^{-1}) and bulk AlH_3 (750 cm^{-1}) obviously are not isolated vibrations of a single Al—H bond.

E. Coverage dependence

Figure 6 displays EEL spectra of the 1825 - (1325-cm^{-1}) band as a function of hydrogen coverage. No coverage dependence could be detected for the position of this or any of the other Al-H (-D) modes. The higher resolution of infrared spectroscopy is required to detect shifts smaller than 25 cm^{-1} . Such measurements should be more feasible on aluminum than on transition metals⁶⁷ because of the more intense metal-hydrogen bands.

Figure 7 is a graphic representation of the peak intensities of the Al-H (-D) bands. A perfect linear correlation is not expected, but the intensity of each peak does increase with coverage. No annealing temperature resulted in exclusively one vibrational feature. It is likely that the population of one site may influence the accessibility of another. Attempts to dose hydrogen intermittently, with intermediate annealing, resulted in the superposition of annealed and unannealed EEL spectra. The accumulated uptake always followed the curve in Fig. 1. We have not yet tried to adsorb a mixture of hydrogen and deuterium. The use of isotopically mixed layers is a standard procedure of decoupling the chemical and physical components of adsorbate-adsorbate interactions.⁶⁸

F. Temperature dependence

Figure 8 shows detailed annealing sequences at low hydrogen (deuterium) coverage. The accumulated results of all such annealing experiments at low coverages are brought together in Fig. 9. It is obvious from these graphs that the 1750-cm^{-1} peak tracks the 750-cm^{-1} peak. Gentle annealing to $130\text{--}150\text{ K}$ populates this state. The higher temperature is required at high coverages ($\Theta=0.50$). It is also clear that the 1825-cm^{-1} band grows with temperature at the expense of the 1125-cm^{-1} band. The “activation energies” of the 1125 - and 1825-cm^{-1} bands are probably the same.

EEL spectra in Fig. 10 were obtained after temperature flashes above 280 K , i.e., after partial recombination and desorption of hydrogen overlayers. From below we see

that the 1750-cm^{-1} peak is fairly symmetric at $<90\text{ K}$ and $\Theta=0.08$. After annealing to 280 K , the 1825-cm^{-1} band dominates with only a slight asymmetry at the low-energy side. Increasing the coverage of the annealed layer broadens the peak, as discussed below. Partial desorption reduces the intensity of the 1825-cm^{-1} band relative to the 1750-cm^{-1} band. The topmost spectra in Fig. 10 are rather fortuitous as to show a dominating 1750-

$(1250\text{-})\text{cm}^{-1}$ peak. More commonly, the 1825- (1325-) and the 1750- (1250-) cm^{-1} peaks vanished with equal intensities.

G. Nature of the 1750- and 750-cm^{-1} species

The suggested assignment of the 1750- and 750-cm^{-1} bands to the A_1 symmetric stretching and scissoring

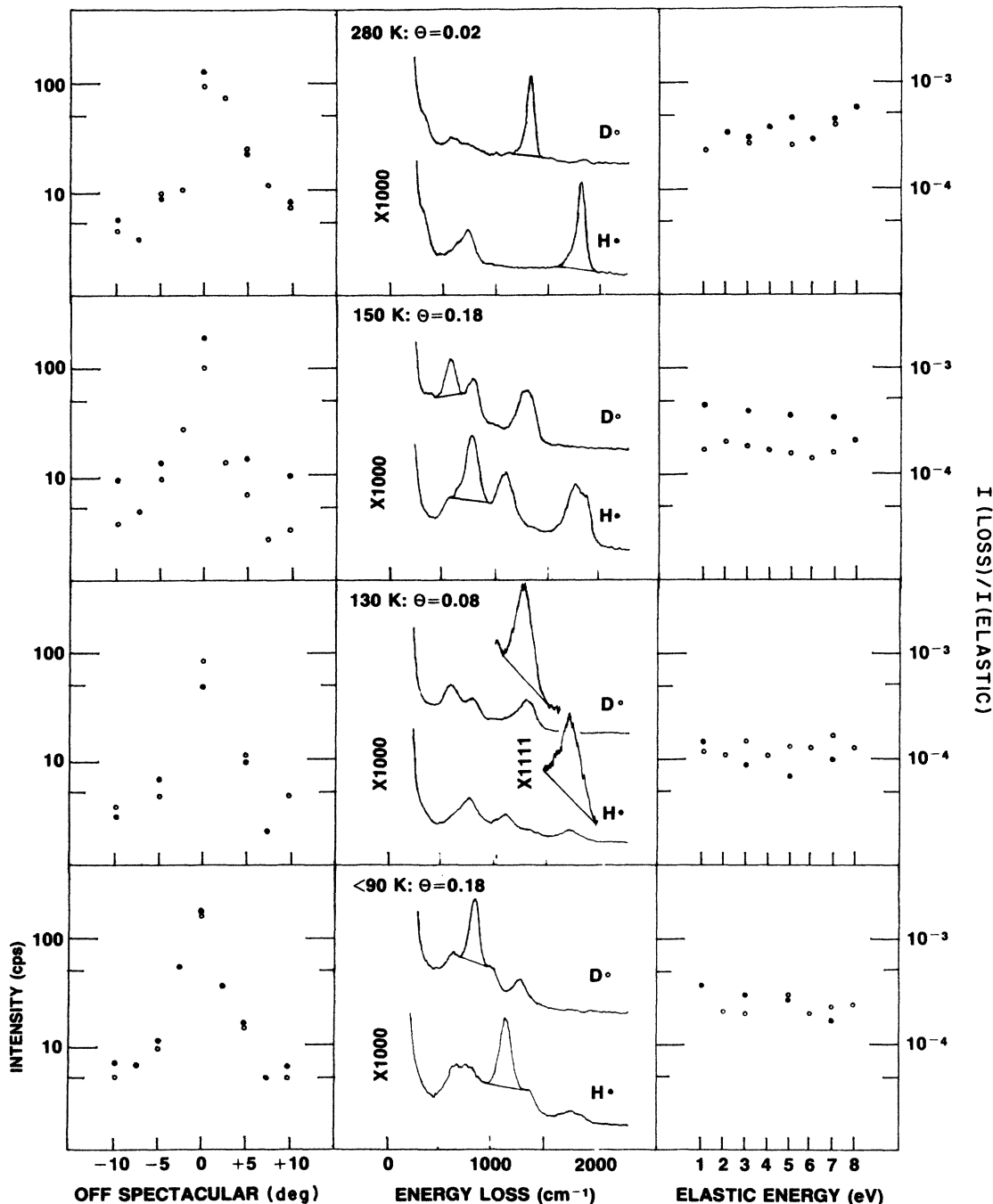


FIG. 5. Angular and elastic energy dependencies of vibrational-loss intensities. The middle panel displays the analyzed area under each peak. The left-hand panel shows the absolute intensity (counts per sec) of each peak as a function of the angle relative to the specular direction. A positive value means a position of the analyzer towards the surface normal. Elastic energy is 5 eV . Specular reflection is obtained around 60° off the surface normal. The right-hand panel shows the relative intensity of each peak in the specular direction vs the elastic electron energy. In both columns, open circles means data for adsorbed deuterium atoms, and solid circles for adsorbed hydrogen atoms.

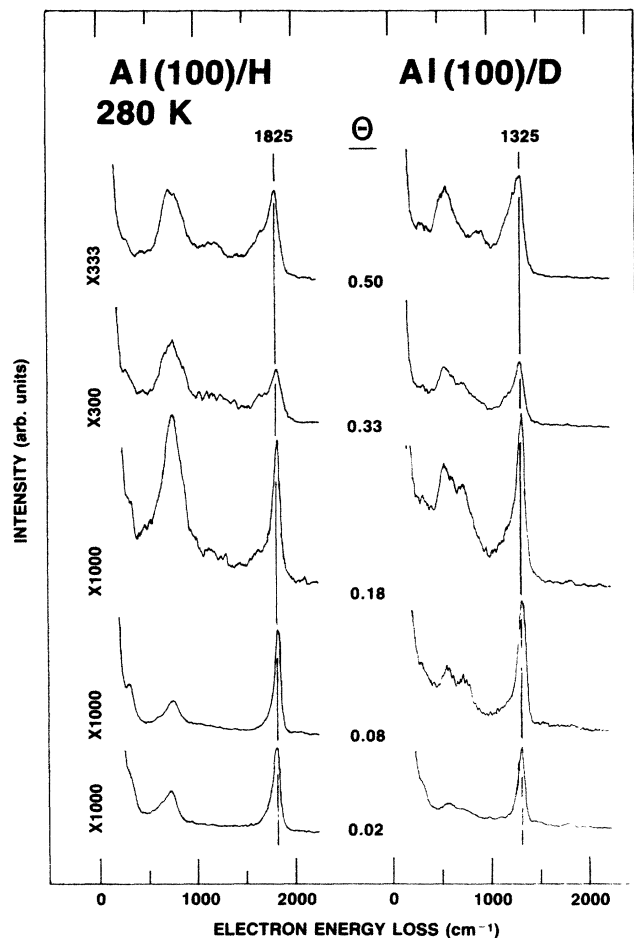


FIG. 6. Coverage dependence of the hydrogen- (deuterium-) induced vibrational loss at 1825 (1325) cm^{-1} . $E_p = 5$ eV. Specular direction.

modes of an aluminum-hydrogen species agrees with all available experimental data. The overall behavior of the 1750- and 750- cm^{-1} species is, however, somewhat irregular and requires further discussion.

A first assumption would be that this species corresponds to the formation of relatively stable "AlH₂" units at defect sites. This would explain the high desorption temperature observed for $\Theta = 0.02$ [Figs. 3(a) and 3(b)], and this correlates nicely with EEL spectra after partial depopulation (Fig. 10). Coverage dependence after annealing to 280 K (Fig. 6) contradicts this model as the sole clue to the 1750- and 750- cm^{-1} bands. The 1750- and 750- cm^{-1} species increase in intensity at high coverages. This is also apparent in Fig. 9, which shows that a higher annealing temperature is required to reach maximum intensity at $\Theta = 0.50$ than at $\Theta < 0.18$. It appears as if we have two sources for intensity in the 1750- and 750- cm^{-1} regions. An imaginative suggestion could be that "AlH₂" species form both at defect sites at low coverages and, more generally, at high coverages. High densities would promote the formation of an overlayer with more than one hydrogen atom per metal atom. This may offset our absolute coverage calibration, which was based on hydrogen evolution from overlayers of alkali hydrides

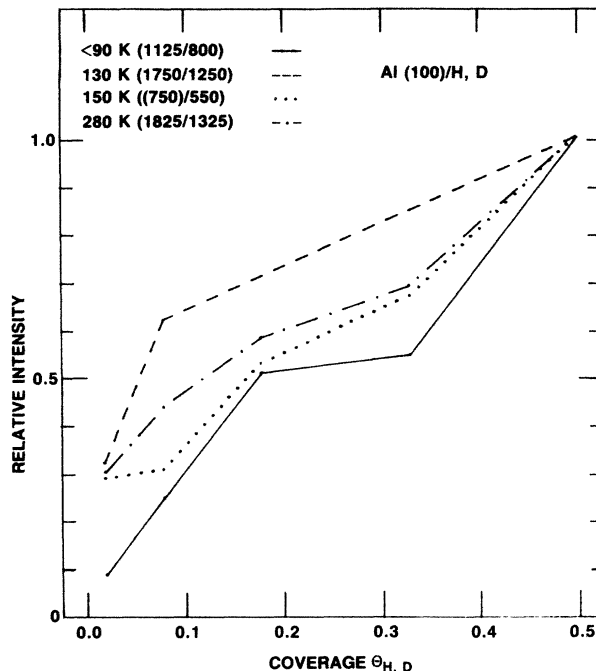


FIG. 7. Relative intensity of vibrational bands vs coverage. The intensity of each peak is normalized to its intensity at $\Theta = 0.50$. The 750- cm^{-1} peak (150 K) is excluded because of the superimposed contribution from Al-O vibrations.

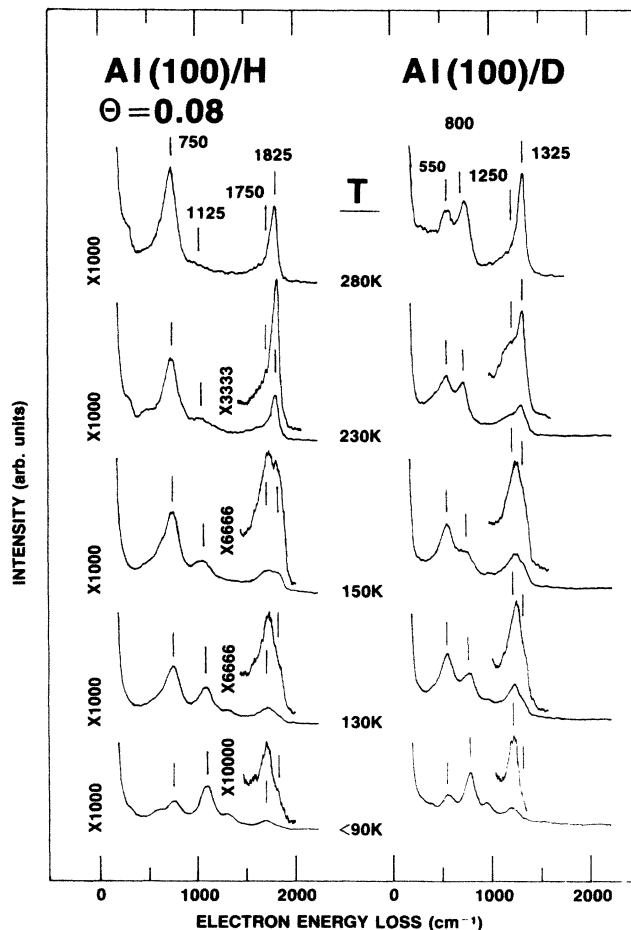


FIG. 8. EEL spectra of Al(100)/H (D) as a function of annealing temperature. No desorption, i.e., constant coverage.

(Fig. 1). $\Theta=2-3$ rather than $\Theta=1$ would then represent saturation. $\Theta=3$ corresponds to the 1:3 stoichiometry of aluminum hydride.

IV. SUMMARY AND CONCLUSIONS

The probability for H—H bond breaking on a clean and defect-free Al(100) surface is less than $1:10^4$ at temperatures below 280 K. Atomic hydrogen recombines and desorbs from Al(100) around 350 K. Surface recom-

bination is probably a limiting factor in hydrogen evolution from the bulk.

We have observed four different Al-H vibrations. A band at 1125 cm^{-1} was assigned to bridge-bonded hydrogen atoms, a second and a third band at 1750 and 1825 cm^{-1} to terminally coordinated species, and a fourth band at 750 cm^{-1} to a bending vibration. The bands at 1750 and 750 cm^{-1} are strongly correlated. All bands are dominated by dipole scattering. The band at 1825 cm^{-1} was tentatively assigned to annealed " $p(1\times 1)$ " is-

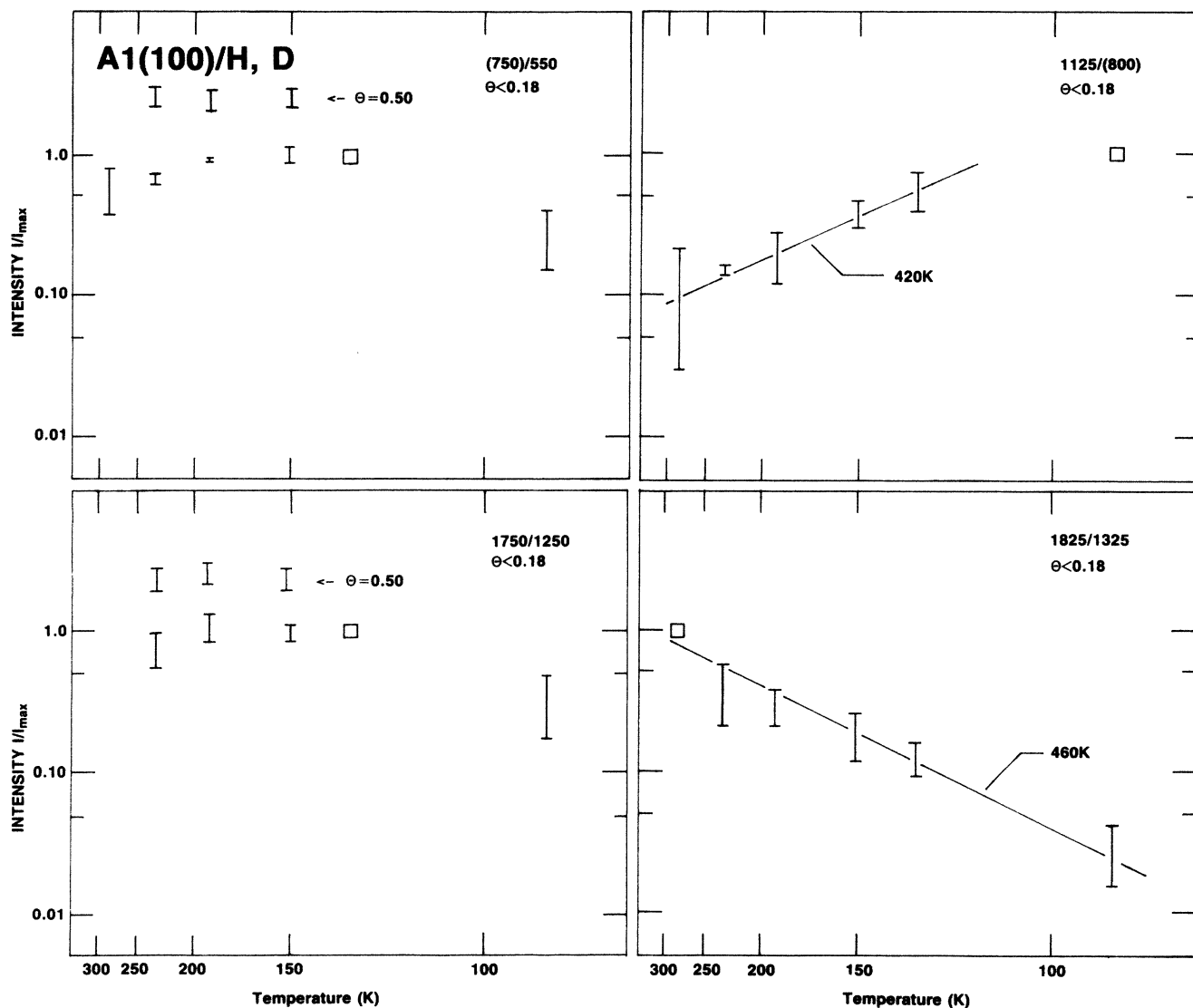


FIG. 9. Intensity of vibrational losses as a function of annealing temperature [$\ln(I/I_{\max})$ vs $1/T$]. I_{\max} is the maximum intensity of each peak, the temperature of which is denoted by a square. The above figures represent the collected data of all measurements at low coverages ($\Theta_{\text{H,D}} < 0.18$). Error bars represent statistical deviations around a mean value. The straight lines represent least-squares fits to the normalized data points and 420 and 460 K the respective slope of each line. The data indicated at $\Theta=0.50$ represent the only observed significant coverage dependence of I/I_{\max} .

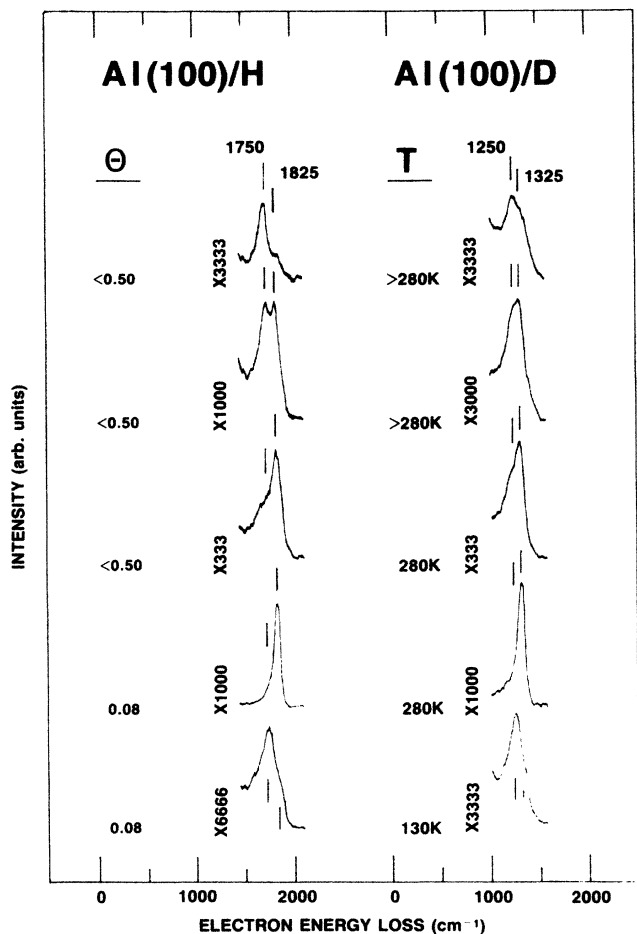


FIG. 10. EEL spectra of Al(100)/H (D) as a function of annealing temperature. From below, (i) $\Theta=0.08$ annealed to 130 K and (ii) 280 K, and (iii) $\Theta=0.50$ annealed to 280 K. The top-most two spectra were obtained after flashes above 280 K, i.e., after fractions of the adatoms had recombined and desorbed.

lands" and the 1750- and 750- cm^{-1} combination to isolated species. Alternatively, the 1825- cm^{-1} band may represent terminally coordinated single atoms and the 1750- and 750- cm^{-1} pair "AlH₂" species. The latter explanation would assign the 750- cm^{-1} peak as a scissoring mode and thus explain its dipole activity.

We have reached the following model for the events following the adsorption of atomic hydrogen on Al(100). Adsorption at <90 K results in the population of bridge sites. Annealing causes depopulation of these sites and the formation of terminal aluminum-hydrogen bonds. The activation energy for this process is around 0.038 eV. The experimental data are consistent with the formation of "AlH₂" species both at defect sites and at high hydrogen coverages.

Future detailed EELS or infrared-absorption measurements are needed to test the above "AlH₂" hypothesis as well as to further narrow the effects of hydrogen-hydrogen interactions as a function of coverage. Valence-band photoemission spectra are also of interest for comparisons with theoretical predictions of the adatom-induced density of states.¹⁶ Even in a differential form such measurements should be less ambiguous than on transition metals, because of the absent *d*-band intensity. Core-level studies are interesting as well and we can expect to see aluminum-surface shifts directly related to aluminum to hydrogen charge transfer without the complexity of interpretations based on *d*-band hybridization.

ACKNOWLEDGMENTS

We acknowledge valuable discussions with D. Cox, R. B. Hall, F. M. Hoffmann, B. K. Kaul, and R. S. Polizzotti, all of Exxon Research and Engineering, and with P. Nordlander, Department of Physics and Astronomy, University of Nashville (Ref. 69).

- ¹M. Suemitsu, T. Kaneko, and N. Miyamoto, *J. Vac. Sci. Technol. A* **5**, 37 (1987).
- ²D. Y. Shih and P. J. Ficalora, *J. Vac. Sci. Technol. A* **2**, 225 (1984).
- ³B. McCarroll and J. R. Anderson, *Surf. Sci.* **17**, 458 (1969).
- ⁴K. Khonde, J. Darville, S. E. Donnelly, and J. M. Gilles, *Appl. Surf. Sci.* **6**, 297 (1980).
- ⁵F. Pellerin, C. Le Gressus, and D. Massignon, *Surf. Sci.* **111**, L705 (1981).
- ⁶O. Nishikawa, T. Yoshimura, and M. Shibata, *Surf. Sci.* **124**, 440 (1983).
- ⁷Ch. Park, M. Bujor, and H. Poppa, *Thin Solid Films* **113**, 337 (1984).
- ⁸P. Breisacher and B. Siegel, *J. Chem. Soc.* **86**, 5053 (1964).
- ⁹D. M. Cox, D. J. Trevor, R. L. Whetten, and A. Kaldor, *J. Phys. Chem.* (to be published).
- ¹⁰T. Upton, *Phys. Rev. Lett.* **56**, 2168 (1986).
- ¹¹P. E. M. Siegbahn, M. R. A. Blomberg, and C. W. Bauschlicher, *J. Chem. Phys.* **81**, 2103 (1984).
- ¹²J. Harris and S. Andersson, *Phys. Rev. Lett.* **55**, 1583 (1985).
- ¹³R. Monnier and J. P. Perdew, *Phys. Rev. B* **17**, 2595 (1978).

- ¹⁴O. Gunnarson, H. Hjelmberg, and B. I. Lundqvist, *Phys. Rev. Lett.* **37**, 292 (1976).
- ¹⁵B. I. Craig and P. V. Smith, *Phys. Status Solidi B* **113**, 747 (1982).
- ¹⁶H. Hjelmberg, *Phys. Scr.* **18**, 481 (1978).
- ¹⁷B. I. Craig, *Phys. Status Solidi B* **114**, 337 (1982).
- ¹⁸R. P. Gupta, *J. Less-Common. Met.* **88**, 299 (1982).
- ¹⁹G. Solt, M. Manninen, and H. Beck, *J. Phys. F* **13**, 1379 (1983).
- ²⁰B. I. Craig, *Phys. Status Solidi B* **115**, 53 (1983).
- ²¹K. Iyakutti, J. L. Calais, and A. H. Tang Kai, *J. Phys. F* **13**, 1 (1983).
- ²²N. Singh and S. P. Singh, *J. Phys. F* **16**, L7 (1986).
- ²³H. F. Ades and A. L. Companso, *Surf. Sci.* **177**, 553 (1986).
- ²⁴P. Nordlander, S. Holloway, and J. K. Nørskov, *Surf. Sci.* **136**, 59 (1984).
- ²⁵B. L. Shaw, *Inorganic Hydrides* (Pergamon, Oxford, 1967), p. 38.
- ²⁶J. W. Turley and H. W. Rinn, *Inorg. Chem.* **8**, 18 (1969).
- ²⁷G. C. Simke, L. C. Walker, F. L. Oetting, and D. R. Stull, *J. Chem. Phys.* **47**, 2759 (1967).

- ²⁸B. Siegel, *J. Am. Chem. Soc.* **82**, 1535 (1960).
- ²⁹J. Paul and F. M. Hoffmann, *J. Phys. Chem.* **90**, 5321 (1986).
- ³⁰J. Paul and F. M. Hoffmann, *Chem. Phys. Lett.* **130**, 160 (1986).
- ³¹J. Paul, *J. Vac. Sci. Technol. A* **5**, 664 (1987).
- ³²J. Paul, *Nature (London)* **323**, 701 (1986).
- ³³J. Paul and F. M. Hoffmann, *J. Chem. Phys.* **86**, 5188 (1987).
- ³⁴J. Paul and F. M. Hoffmann, *Surf. Sci.* **194**, 419 (1988).
- ³⁵F. Greuter and E. W. Plummer, *Solid State Commun.* **48**, 37 (1983).
- ³⁶L. Chan and G. L. Griffin, *Surf. Sci.* **145**, 185 (1984).
- ³⁷See, e.g., P. Feulner and D. Menzel, *Surf. Sci.* **154**, 465 (1985).
- ³⁸M. G. Cattania, V. Penka, R. J. Behm, K. Christmann, and G. Ertl, *Surf. Sci.* **126**, 382 (1983).
- ³⁹We are not aware of any monograph on surface isotope effects. For effects in three dimensions, see, e.g., L. Melander and W. H. Saunders, *Reaction Rates of Isotopic Molecules* (Kruger, Melbourne, FL, 1987).
- ⁴⁰J. Paul and R. B. Hall (unpublished).
- ⁴¹J. E. Muller and J. Harris, *Phys. Rev. Lett.* **53**, 2493 (1984).
- ⁴²W. Eichenauer, K. Hattenbach, and A. Pebler, *Z. Metallkd.* **52**, 682 (1961).
- ⁴³K. Papp and E. Kovacs-Csentyi, *Scr. Metall.* **11**, 921 (1977).
- ⁴⁴K. L. Wilson and L. G. Haggmark, *Thin Solid Films* **63**, 283 (1979).
- ⁴⁵S. M. Myers, F. Besenbacher, and J. K. Nørskov, *J. Appl. Phys.* **58**, 1841 (1985).
- ⁴⁶S. M. Myers, P. Nordlander, F. Besenbacher, and J. K. Nørskov, *Phys. Rev. B* **33**, 854 (1986).
- ⁴⁷J. E. Crowell, J. G. Chen, and J. T. Yates, Jr., *Surf. Sci.* **165**, 37 (1986).
- ⁴⁸K. P. Slater and G. Herzberg, *Molecular Spectra and Molecular Structure IV. Constants of Diatomic Molecules* (Van Nostrand/Reinhold, New York, 1979).
- ⁴⁹E. R. Lippincott, *J. Chem. Phys.* **17**, 1351 (1949).
- ⁵⁰E. G. Hoffmann and G. Schomburg, *Z. Electrochem.* **61**, 1101 (1957).
- ⁵¹H. Roszinski, R. Dautel, and W. Zeil, *Z. Phys. Chem. Neue Folge* **36**, 26 (1963).
- ⁵²H. Hjelmberg, *Surf. Sci.* **81**, 539 (1979).
- ⁵³C. Nyberg and C. G. Tengstål, *Phys. Rev. Lett.* **50**, 1680 (1983).
- ⁵⁴P. Nordlander and S. Hölmstrom, *Surf. Sci.* **159**, 443 (1985).
- ⁵⁵P. A. Karlsson, A. S. Martensson, S. Andersson, and P. Nordlander, *Surf. Sci.* **175**, L759 (1986).
- ⁵⁶CO island formation on different metal surfaces has been concluded from infrared-absorption measurements [F.M. Hoffmann, *Surf. Sci. Rep.* **3**, 107 (1983)].
- ⁵⁷H clustering on metals; see, e.g., J. A. Prybyla, P. J. Estrup, S. C. Ying, Y. J. Chabal, and S. B. Christman, *Phys. Rev. Lett.* **58**, 1877 (1987).
- ⁵⁸M. W. Howard, U. A. Jayasooriya, S. F. A. Kettle, D. B. Powell, and N. Sheppard, *J. Chem. Soc. Chem. Commun.* **18** (1979).
- ⁵⁹J. Kirtley, D. J. Scalapino, and P. K. Hansma, *Phys. Rev. B* **14**, 3177 (1976).
- ⁶⁰J. Igalson and J. G. Adler, *Phys. Rev. B* **28**, 4970 (1983).
- ⁶¹S. Gauthier, S. deCheveigne, J. Klein, and M. Belin, *Phys. Rev. B* **29**, 1748 (1984).
- ⁶²P. A. Thiry, J. J. Pireaux, M. Lehr, and R. Caudano, *J. Vac. Sci. Technol. A* **3**, 1439 (1985).
- ⁶³R. H. Hauge, J. W. Kauffman, and J. L. Margrave, *J. Am. Chem. Soc.* **102**, 6005 (1980).
- ⁶⁴See, e.g., W. Ho, N. J. DiNardo, and E. W. Plummer, *J. Vac. Sci. Technol.* **17**, 134 (1980).
- ⁶⁵For W(100)/H EELS, see J. P. Woods and J. L. Erskine, *Phys. Rev. Lett.* **55**, 2595 (1985); R. F. Willis, in *Vibrational Spectroscopy of Adsorbates*, edited by R. F. Willis (Springer, Berlin, 1980), p. 23.
- ⁶⁶H. Ibach and D. L. Mills, *Electron Energy Loss Spectroscopy* (Academic, New York, 1982).
- ⁶⁷For W(100)/H infrared-absorption spectroscopy, see Y. Chabal, *J. Vac. Sci. Technol. A* **4**, 1324 (1986), cf. Ref. 65.
- ⁶⁸See, e.g., Refs. 53–55 for hydrogen, and B. N. J. Persson and R. Ryberg, *Phys. Rev. B* **24**, 6954 (1981), for carbon monoxide.
- ⁶⁹J. Paul, F. M. Hoffmann, and P. Nordlander (unpublished).